Bioorganic & Medicinal Chemistry Letters 30 (2020) 127536

Contents lists available at ScienceDirect

Bioorganic & Medicinal Chemistry Letters

journal homepage: www.elsevier.com/locate/bmcl

Discovery of ONO-8590580: A novel, potent and selective $GABA_A$ α_5 negative allosteric modulator for the treatment of cognitive disorders

A. Lewis[a], A. Beresford[a], M.S. Chambers[a], G. Clark[a], D.C. Hartley[a], K.L. Hirst[a], M. Higashino[b], S. Kawahadara[b], M. Nakanishi[b], T. Saito[b], A. Imagawa[b], H. Habashita[b], S. Maidment[a], A.M. Macleod[a], A.P. Owens[a], A. Rae[a,*], C. Rouse[a], G. Wishart[a]

[a] Charles River Discovery Research Services, Chesterford Research Park, Little Chesterford, Essex CB10 1XL, United Kingdom
[b] Ono Pharmaceutical Co. Ltd., Minase Research Institute, Shimamoto-cho, Mishima-gun, Osaka 618-8585, Japan

ARTICLE INFO

Keywords:
GABAA α5
Negative allosteric modulator
Cognition enhancement
ONO-8590580

ABSTRACT

The identification and SAR development of a series of negative allosteric modulators of the $GABA_A$ α5 receptor is described. This novel series of compounds was optimised to provide analogues with high $GABA_A$ α5 binding affinity, high α5 negative allosteric modulatory activity, good functional subtype selectivity and low microsomal turnover, culminating in identification of **ONO-8590580**.

$GABA_A$ receptors are pentameric membrane proteins that gate chloride ions in response to the binding of γ-aminobutyric acid (GABA). $GABA_A$ ion channels containing the α5-subunit ($GABA_A$ α5) are highly expressed in the hippocampus, a key area of the brain associated with cognitive processing,[1] and it has previously been shown that $GABA_A$ α5 negative allosteric modulators (NAMs) are efficacious in models thought to reflect pro-cognitive properties in rodents.[2,3,4] Furthermore, mice with a disrupted α5 gene (α5 −/− mice) show improved performance in the spatial learning water maze test compared with wild-type mice.[5] Taken together, these data support the hypothesis that $GABA_A$ α5 NAMs may offer therapeutic potential for the treatment of cognitive disorders, such as Down's syndrome and Alzheimer's disease. However, in adopting this therapeutic approach it is essential that the $GABA_A$ α5 NAM should demonstrate binding or functional selectivity for the $GABA_A$ α5-subunit, as negative modulation of other $GABA_A$ subunits expressed in the CNS can lead to unwanted pro-convulsant ($GABA_A$ α1) or anxiogenic ($GABA_A$ α2 or $GABA_A$ α3) effects.[6,7]

This approach to cognition enhancement has attracted considerable attention in recent years, with several $GABA_A$ α5 NAMs, including α5IA, MRK-016 and basmisanil reaching clinical evaluation (Fig. 1).[2,3,4,8,9] In Down's Syndrome subjects, basmisanil did not demonstrate efficacy in the cognition primary end-points[10] and has subsequently been withdrawn from Roche's pipeline. Merck's α5IA was evaluated for cognitive performance in ethanol-impaired volunteers, and those subjects on drug demonstrated a significant improvement in a list recall experiment compared to those on placebo.[11] However, progression of α5IA was terminated due to renal toxicity in pre-clinical species.[12] MRK-016 entered Phase I clinical evaluation but was subsequently terminated due to poor tolerability in elderly patients and variable pharmacokinetics.[2]

In order to identify starting points for a $GABA_A$ α5 NAM drug discovery program, approximately 124,000 compounds were screened from the Charles River Laboratories screening collection, at a concentration of 10 μM, in both receptor binding and FLIPR functional assays against human $GABA_A$ α5β3γ2 expressed in HEK293 cells. In the high throughput screen (HTS), receptor binding was assessed by measuring the inhibition of binding of commercially available [^{3}H]-Ro15-1788 ([^{3}H]-flumazenil), and in the FLIPR assays an EC_{20} concentration of GABA was co-applied with the test compound, in order to determine the functional response.[13] Following the HTS, 525 compounds showed > 40% inhibition at 10 μM in both the binding and FLIPR assays, which were progressed to determination of binding Ki and concentration-response functional activity against $GABA_A$ α5β3γ2. In the FLIPR assay, 26 of the 525 compounds demonstrated an IC_{50} value against $GABA_A$ α5 of < 1 μM, which were progressed to evaluation of functional selectivity against the $GABA_A$ α1, α2 and α3 subtypes. A promising hit from this screening exercise was imidazopyridine **1**, which demonstrated moderate binding affinity, significant negative modulation of the GABA response at the $GABA_A$ α5 receptor, and minimal effect on the GABA response at the α1, α2 and α3 subtypes (Table 1). However, **1** was rapidly metabolised in both rat and human liver microsomes. Consequently, a program of work was initiated

* Corresponding author.
E-mail address: alastair.rae@crl.com (A. Rae).

https://doi.org/10.1016/j.bmcl.2020.127536
Received 11 May 2020; Received in revised form 28 August 2020; Accepted 31 August 2020
Available online 06 September 2020
0960-894X/

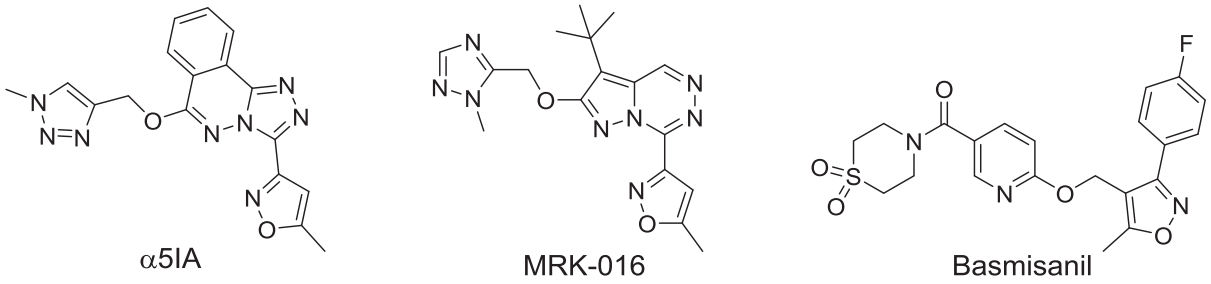

Fig. 1. *α5IA, MRK-016 and Basmisanil.*

Table 1
Binding affinity, functional efficacy and microsomal stability data for imidazopyridine **1**.

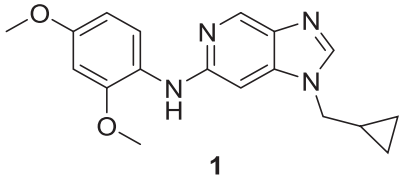

1

$GABA_A$ α5	Efficacy[1] (%)				Half-life in liver microsomes (min)	
Ki (nM)[2]	α5	α1	α2	α3	Rat	Human
76	−42	−1	−7	−6	< 5	14

[1]Effect of 1 μM compound on the current induced by the EC_{20} concentration of GABA on human recombinant $GABA_A$ α5, α1, α2, or α3 subunits expressed in HEK293 cells. Current recordings were performed using PatchXpress (Molecular Devices, LLC). A detailed protocol for the efficacy assays is described in the Supplementary Information.
[2]*In vitro* binding affinity at the human $GABA_A$ α5β3γ2 receptor, measured using a scintillation proximity assay (radioligand [^{3}H]-Ro15-1788). A detailed protocol for this binding assay is described in the Supplementary Information.

around **1**, targeting increased $GABA_A$ α5 receptor affinity and improved microsomal stability, with retention of $GABA_A$ α5 functional selectivity. Importantly, analogues from the imidazopyridine series exemplified by **1** did not show any binding selectivity for α5 versus the other main $GABA_A$ subtypes, and consequently the program strategy was to invoke subtype selectivity in a functional manner.

The electron-rich dimethoxyphenyl substituent in **1** was surmised to be a potential metabolic liability, with susceptibility to *O*-demethylation and oxidation of the aryl ring. Therefore, the SAR around the aryl group was investigated as a priority, with emphasis on reduction of electron density in the ring and/or lowering of the molecule's lipophilicity, targeting analogues with retained or improved binding affinity and improved microsomal stability. Some specific examples synthesised for the dimethoxy replacement program are shown in Table 2. Removal of one or both of the methoxy substituents to lower electron density on the ring (compounds **2** and **3**) resulted in a significant loss of binding affinity. Aliphatic substituents such as cyclopropylmethyl (compound **4**) were not tolerated. An alternative electron-donating substituent that afforded a reduction in lipophilicity was the morpholine of analogue **5**, which had similar binding affinity to **1** and somewhat improved metabolic stability, although this benefit came with a cost of reduced $GABA_A$ α5 negative allosteric modulation. Introducing the more polar carboxamide group (**6**) retained the acceptable $GABA_A$ α5 inverse agonism of **1** but had 4-fold weaker $GABA_A$ α5 affinity. However, by incorporating the hydrogen-bond acceptor group in a fused bicycle to afford the benzoxazole **7** or benzoxazinone **8** provided analogues with very encouraging *in vitro* profiles. Most notable was the benzoxazinone **8**, which had a reasonable functional selectivity profile and, importantly, 4-fold higher $GABA_A$ α5 binding affinity and significantly improved rat and human microsomal stability compared to **1**. Consequently, **8** became the focus of further optimisation.

A variety of structural modifications to the benzoxazinone substituent were investigated and key analogues are shown in Table 3. The first set of compounds **9–14** were designed to probe the structure–activity relationship around the oxazinone ring. The secondary amide **9** retained high stability following incubation with human liver microsomes, and also provided improved rat microsomal stability, possibly as a result of eliminating *N*-de-methylation as a route of metabolism. However, this change also resulted in an undesirable elevation of the levels of negative modulation at α1 and α2. The isomeric benzoxazinone **10** maintained a similar profile to **8**, albeit with 4-fold reduced binding affinity, whereas the ring contraction analogue – benzoxazolone **11** – suffered from an unacceptable functional selectivity profile, and inferior metabolic stability compared to **8** or **9**. Lactam **12** retained good binding affinity but was a positive modulator at α1. Introduction of a methyl group adjacent to the carbonyl group of the oxazinone ring to afford compound **13** was well tolerated for GABAA α5 affinity and enhanced rat microsomal stability compared to the parent compound **8**. The difluorinated benzoxazinone **14** afforded an excellent functional selectivity profile with good affinity against $GABA_A$ α5, although microsomal stability was sub-optimal. To assist with identification of the main routes of metabolism in this series and inform the design of more stable analogues, benzoxazinone **14** was subjected to a metabolite ID study in human liver microsomes. This study indicated de-methylation of the amide and oxidation of either the aryl ring or imidazopyridine scaffold as primary metabolic pathways. A key strategy towards investigating the potential for oxidative aryl metabolism of the benzoxazinone group was to reduce the electron density of the phenyl ring by replacing phenyl with pyridyl to afford the azabenzoxazinones **15–17**. This approach proved to be successful, with all three isomers retaining high stability in the presence of human liver microsomes, and enhanced stability in rat liver microsomes compared to their phenyl counterpart **8**. Of these three isomers it was azabenzoxazinone **17** that showed the best overall profile, with high stability in both human and rat liver microsomes, high $GABA_A$ α5 negative allosteric modulation and no significant functional response against the other key $GABA_A$ subtypes. Consequently, this optimised substituent was retained in a further program of work around the imidazopyridine scaffold, with the objective of increasing binding affinity to maximise the likelihood of achieving high receptor occupancy *in vivo*.

Earlier investigation of SAR in the 1*H*-imidazo[4,5-*c*]pyridine series had shown that modifications to the imidazole ring such as nitrogen deletion or substitution at *C*2 were not tolerated, and that alternative substituents to cyclopropyl at *N*1 did not confer improvements to the overall profile. Hence, subsequent analogue synthesis was aimed towards retaining the attractive microsomal stability and $GABA_A$ α5 functional selectivity profile of compound **17** and improving the α5 affinity by evaluating modifications to the six-membered ring of the imidazopyridine scaffold (Table 4).

Methylation (**18**) at the *C*4 position of the scaffold maintained

Table 2
In vitro data for selected C6-substituted imidazopyridines.

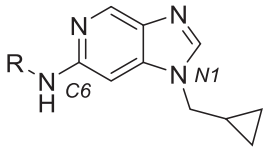

R	ID	cLogP	$GABA_A$ α5 Ki (nM)	Efficacy (%)				Half-life in liver microsomes (min)	
				α5	α1	α2	α3	Rat	Human
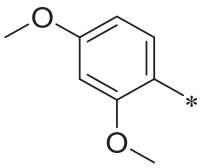	**1**	4.0	76	−42	−1	−7	−6	< 5	14
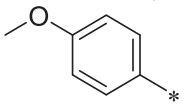	**2**	3.8	459	−43	−20	−20	3	–	–
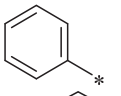	**3**	3.5	972	−26	–	–	–	–	–
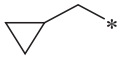	**4**	3.1	> 15,000	–	–	–	–	–	–
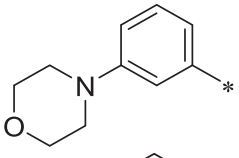	**5**	3.1	119	−26	–	–	–	36	23
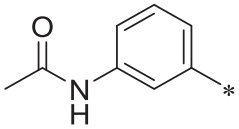	**6**	2.9	319	−44	−11	−11	−11	–	–
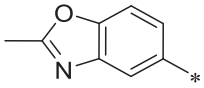	**7**	3.2	85	−42	−16	−10	−6	10	38
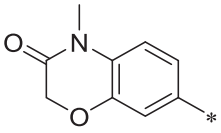	**8**	2.8	17	−46	−8	−2	−17	19	> 100

binding affinity relative to **17**, but the functional selectivity profile for this 4-alkylated 1*H*-imidazo[4,5-*c*]pyridines was inferior. The isomeric 3*H*-imidazo[4,5-*b*]pyridine core exemplified in analogues **19**–**21** also provided enhanced $GABA_A$ α5 binding affinity (Ki 2–19 nM) compared to **17**, but their functional or microsomal stability profiles were less attractive.

Introducing further polarity into the central core to afford the 9*H*-purine scaffolds provided compounds **22** and **23** which had favourable α5 affinity compared to **17**, but sub-optimal microsomal stability and $GABA_A$ α5 functional selectivity profiles.

To complete SAR development around the scaffold, an array of benzimidazoles was also synthesised. Within this sub-series, the 5-trifluoromethoxy- (**24**) 5-fluoro- (**25**) and 4-methyl-5-fluoro analogues demonstrated improved $GABA_A$ α5 binding affinity compared to **17**, the most notable of which was **24**, which exhibited sub-nanomolar $GABA_A$ α5 affinity (Ki 0.5 nM). Unfortunately, compound **24** demonstrated significant negative modulation against the $GABA_A$ α2 (−16%) and $GABA_A$ α3 (−31%) subtype, thus rendering it liable to the undesired side-effects demonstrated by non-selective $GABA_A$ NAMs.[6,7] In contrast, **25** had high $GABA_A$ α5 inverse agonism and essentially negligible functional activity at either α1, α2 or α3. However, compound **25** exhibited a relatively poor microsomal stability profile. As had been observed when comparing the purines **22** and **23**, *C4*-methylation also enhanced metabolic stability in the benzimidazole series, with compound **26** demonstrating improved rat microsomal stability compared to **25**. Indeed, **26** had an encouraging *in vitro* profile, with a $GABA_A$ α5 Ki of 7 nM, high α5 inverse agonism (−49%) and good functional selectivity over the other $GABA_A$ subtypes.

As the results in Table 4 demonstrate, the substituted benzimidazoles (**24**–**26**) exhibited high $GABA_A$ α5 binding affinity and $GABA_A$ α5 NAM activity, and in the case of **25** and **26**, a good functional selectivity profile. Consequently, in an effort to understand the major routes of metabolism in this class, the 5-fluorobenzimidazole **25** was subjected to a metabolite ID study. As previously observed for the 1*H*-imidazo[4,5-*c*]pyridine **14**, the major *in vitro* metabolites for benzimidazole **25** were derived from *N*-dealkylation or oxidation of the azabenzoxazinone unit. Hence, further efforts were instigated to find replacements for the *C*6 substituent, focussing on the 4-methyl-5-fluorobenzimidazolyl (**26**),

Table 3
In vitro data for selected analogues incorporating modifications to the C6 benzoxazinone substituent.

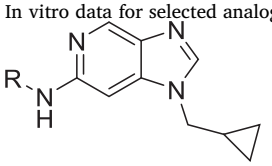

R	ID	$GABA_A$ α5 Ki (nM)	Efficacy (%)				Half-life in liver microsomes (min)	
			α5	α1	α2	α3	Rat	Human
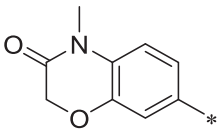	**8**	17	−46	−8	−2	−17	19	> 100
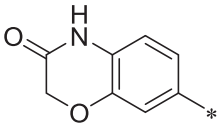	**9**	42	−48	−18	–32	−18	59	> 100
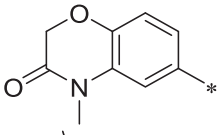	**10**	65	−41	0	−10	−13	25	77
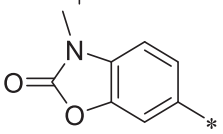	**11**	62	−50	−31	–	−21	8	73
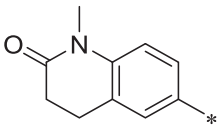	**12**	16	−38	+32	–	+13	25	70
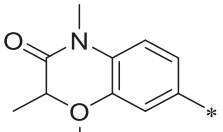	**13**	17	−40	+19	+54	+60	55	> 100
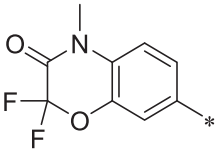	**14**	11	−55	+1	−1	+12	22	52
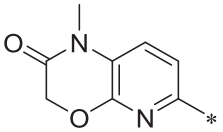	**15**	45	−46	−22	−39	−27	39	93
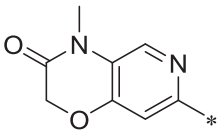	**16**	11	−45	−45	−27	−26	45	> 100
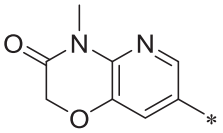	**17**	38	−52	0	−8	−8	> 100	> 100

and 4-methyl 3*H*-imidazo[4,5-*b*]pyridyl (**20**) cores, both of which had previously demonstrated high α5 binding affinity, and strong negative modulation against α5.

As bicyclic systems to replace the benzoxazinone had been investigated earlier in the campaign, an alternative approach to *C*6 substituent design was taken in which this substituent was replaced with a variety of pendent heterocycles, in a manner that allowed retention of a hydrogen-bond acceptor atom in a similar region of space to that of the oxazinone carbonyl. As shown in Table 5, this strategy provided multiple analogues that retained high $GABA_A$ α5 binding affinity and high $GABA_A$ α5 NAM activity. Within this series of compounds, it was **ONO-8590580** that emerged as the compound with the best overall *in vitro*

Table 4
In vitro data for different scaffolds.

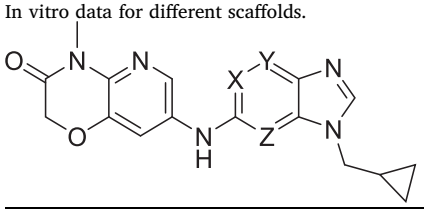

	ID	$GABA_A$ α5 Ki (nM)	Efficacy (%)				Half-life in liver microsomes (min)	
			α5	α1	α2	α3	Rat	Human
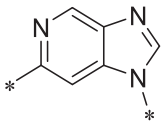	**17**	38	−52	0	−8	−8	> 100	> 100
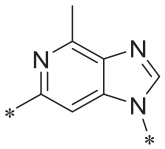	**18**	58	−50	−16	−15	+5	> 100	> 100
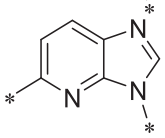	**19**	19	−33	+17	−2	nd	7	14
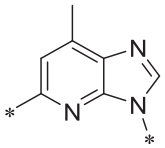	**20**	4	−57	+21	+2	+2	22	29
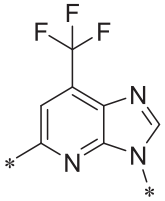	**21**	2	−43	+36	+5	+24	67	63
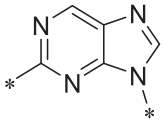	**22**	17	−33	+9	+7	+3	18	55
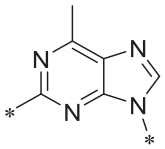	**23**	14	−43	+15	−9	+20	55	> 100
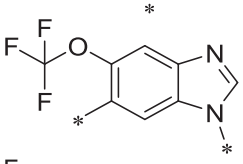	**24**	0.5	−55	−8	−16	−31	33	10
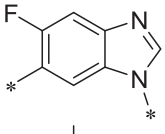	**25**	12	−47	1	−7	0	17	32
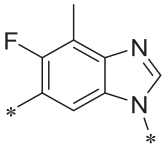	**26**	7	−49	+3	−10	−7	55	39

Table 5
Data for selected analogues incorporating pendent heterocycles.

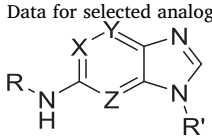

R	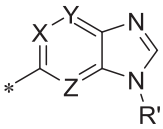	ID	α5 Ki (nM)	Efficacy (%)				Half-life in liver microsomes (min)	
				α5	α1	α2	α3	Rat	Human
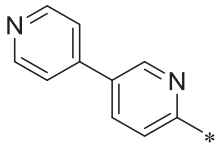	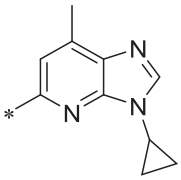	**27**	7	−55	−5	−11	−11	24	46
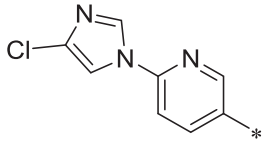	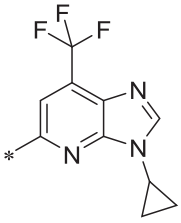	**28**	4	−42	−6	−19	−18	74	> 100
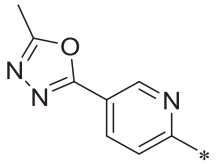	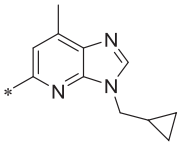	**29**	2	−52	−21	−8	−10	> 100	> 100
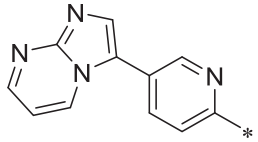	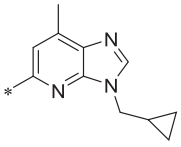	**30**	1	−50	−11	−10	−5	28	41
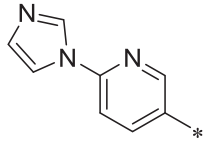	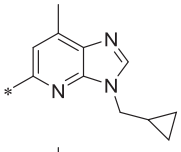	**31**	15	−50	−8	−4	−3	20	40
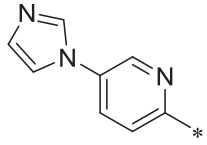	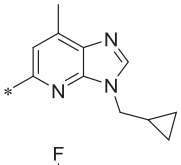	**32**	2	−42	−10	−1	6	27	> 99
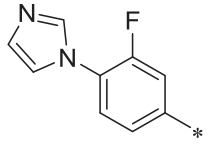	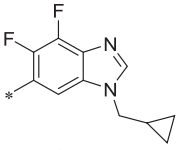	**33**	2	−54	−24	−10	−24	44	> 100
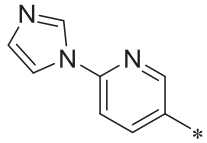	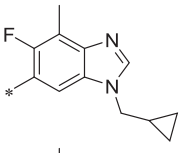	**34**	9	−50	−11	−17	−15	18	> 100
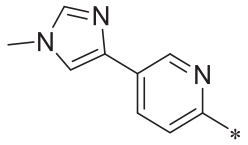	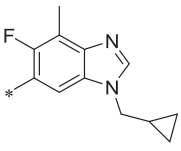	**ONO-8590580**	8	−50	−2	+5	−6	> 100	60

Table 6
In vitro and *in vivo* data for ONO-8590580.

ID	α5 Ki (nM)	α5 efficacy (%)	MDCK-MDR1 P_{app} (x 10^{-6} cms^{-1})/efflux ratio	Plasma protein binding, rat (% bound)	Brain homogenate binding, rat (% bound)	*In vivo* receptor occupancy of $GABA_A$ α5 receptors in rat brain (%)[1]
ONO-8590580	8	−50	47 / 0.9	93	96	71

[1]Occupancy of the binding site of rat brain $GABA_A$ α5 was measured using an *in vivo* [^{3}H]-Ro15-4513 binding assay (n = 3–4 in each group). [^{3}H]-R015-4513 is a $GABA_A$ α5-specific binding radioligand. **ONO-8590580** was orally administered at 10 mg/kg 1 h before sacrifice. [^{3}H]-Ro15-4513 was intravenously administered 10 min before sacrificing the rats. The amount by which **ONO-8590580** reduced the specific binding of [^{3}H]-Ro15-4513 relative to the binding in non-treated rats was defined as the occupancy.[14]

Table 7
In vivo rat PK parameters for **ONO-8590580**.

Route[1]	Dose (mg/kg)	V_{ss} (L/kg)	C_{max} (ng/mL)	$t_{1/2}$ (min)	AUC_{inf} (μg/mL.min)	Cl (mL/min/kg)	%F[2]
i.v.	0.44	1.7	278	72	24	18	–
p.o.	3	–	520	131	107	–	65

[1]Vehicle for *i.v.*: DMSO:Cremophor:water (10:10:80). Vehicle for po: 0.5% w/v methylcellulose in water.
[2]Bioavailability.

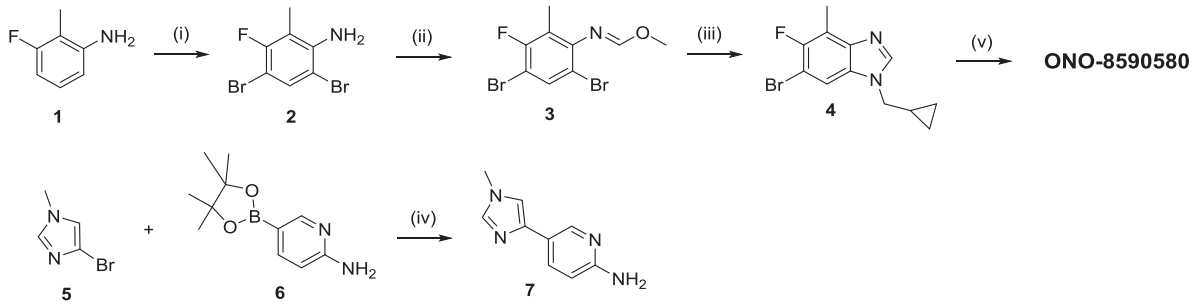

Scheme 1. Synthetic route to **ONO-8590580**. (i) Benzyltrimethylammonium tribromide, CH_2Cl_2/MeOH (97%); (ii) Trimethylorthoformate, p-TsOH, reflux; (iii) cyclopropylmethylamine, CuI, DBU, DMSO, 120 °C (62% for 2 steps); (iv) $Pd(PPh_3)_4$, Na_2CO_3, DMF/water, 100 °C (55%); (v) **7**, Pd_2dba_3, xantphos, Cs_2CO_3, dioxane, 90 °C (27%).

profile. **ONO-8590580** has very high negative allosteric modulatory activity against $GABA_A$ α5 and high α5 binding affinity. Moreover, it demonstrates an excellent functionally selectivity profile, with essentially no functional activity against the other subtypes, high rat microsomal stability and good human microsomal stability. Consequently, **ONO-8590580** was taken forward for further ADME evaluation and *in vivo* profiling.

As shown in Table 6, **ONO-8590580** exhibited good cell permeability and only a modest efflux ratio in the MDCK-MDR1 cell line, consistent with potential for brain penetration. Rat plasma protein binding and rat brain homogenate binding were 93% and 96%, respectively, providing confidence that good oral exposure would achieve a satisfactory level of target engagement in the brain.

As shown in Table 7, in rats **ONO-8590580** had modest plasma clearance (18 mL/min/kg) and 65% oral bioavailability, following *i.v.* and oral dosing at 0.44 mg/kg and 3 mg/kg, respectively. Moreover, after dosing at 10 mg/kg *p.o.* **ONO-8590580** afforded 71% occupancy of $GABA_A$ α5 receptors in the rat hippocampus (Table 6).[14] **ONO-8590580** was also assessed for functional response against the hERG ion channel, for which it demonstrated an IC_{50} of 11 μM.

As reported previously by Kawaharada et al.,[14] **ONO-8590580** dose-dependently reversed MK-801-induced cognitive deficit in the rat passive avoidance and 8-arm radial maze tests, and did not elicit anxiogenic or pro-convulsant side-effects when administered at doses that provide high $GABA_A$ receptor occupancy in the brain.

The synthesis of **ONO-8590580** is shown in Scheme 1, and was accomplished using a convergent strategy, *via* a Buchwald-Hartwig coupling of the 6-bromobenzimidazole **4** and the substituted 2-aminopyridine **7**. A key step was the copper-mediated formation of the benzimidazole ring (**3** → **4**).[15]

In summary, optimisation of the hit imidazopyridine **1** focussing on modification of physicochemical properties and utilising metabolite ID studies to drive improvements in metabolic stability has led to identification of the benzimidazole **ONO-8590580**. This compound displayed good binding affinity, high negative modulation of the $GABA_A$ α5 receptor subtype, an excellent functional selectivity profile and, as previously reported,[14] is efficacious in two *in vivo* models of cognition enhancement. Consequently, it is our belief that **ONO-8590580** is a valuable tool compound to pre-clinically evaluate the pharmacological effects of selectively negatively modulating the functional response of the $GABA_A$ α5 receptor subtype.

Declaration of Competing Interest

The authors declare that they have no known competing financial interests or personal relationships that could have appeared to influence the work reported in this paper.

Appendix A. Supplementary data

Supplementary data to this article can be found online at https://doi.org/10.1016/j.bmcl.2020.127536.

References

1. Quirk K, Blurton P, Fletcher S, et al. *Neuropharmacology.* 1996;35:1331–1335.
2. Atack JR, Maubach KA, Wafford KA, et al. *J Pharmacol Exp Ther.* 2009;331(2):470–484.
3. Dawson GR, Maubach KA, Collinson N, et al. *J Pharmacol Exp Ther.* 2006;316:1335–1345.
4. Ballard TM, Knoflach F, Prinssen E, et al. *Psychopharmacology.* 2009;202:207–223.

5. Collinson N, Kuenzi FM, Jarolimek W, et al. *J Neurosci.* 2002;22(13):5572–5580.
6. Vergnes M, Boehrer A, He X, et al. *Epilepsy Res.* 2001;47:43–53.
7. Horowski R, Dorrow R. *Psychopharmacology.* 2002;162:223–224.
8. Sternfeld F, Carling RW, Jelley RA, et al. *J Med Chem.* 2004;47(9):2176–2179.
9. https://clinicaltrials.gov/ct2/show/NCT02024789, Accessed 26 Nov 2019.
10. http://www.edsa.eu/roche-clematis-trial-discontinued/, Accessed 25 Aug 2020.
11. Nutt DJ, Besson M, Wilson SJ, Dawson GR, Lingford-Hughes AR. *Neuropharmacology.* 2007;53(7):810–820.
12. Atack JR. *Pharmacol Ther.* 2010;125(1):11–26.
13. Protocols for the α5 SPA binding and FLIPR assay used in the high throughput screen are described in the Supplementary Information.
14. Kawaharada S, Nakanishi M, Nakanishi N, et al. *J Pharmacol Exp Ther.* 2018;366:58–65.
15. Hirano K, Biju AT, Glorius F. *J Org Chem.* 2009;74:9570–9572.